

The analysis of high efficiency multi-junction solar cells architecture using a diffractive optical element as the spectrum splitting solar concentrator

Qingli Huang^{1, a}, Jinze Wang^{2, b}, Jianyao Hu^{1, c}, Huawei Xu^{1, d}, Qi Peng^{1, e},
Chunxu Jiang^{1, f}, Qunxing Liu^{1, g}

¹The Fifth Electronics Research Institute of Ministry of Industry and Information Technology,
Guangzhou, Guangdong, 510610, China

²Brion Technologies (Shenzhen) Co. Ltd, NanShan District, Shenzhen, Guangdong, 518057,
China

^ahuangqingli@ceprei.biz, ^bsimpletruth@163.com, ^chujianyao@ceprei.biz, ^dxhw@ceprei.biz,
^epengqi@ceprei.biz, ^fjcx@ceprei.biz, ^glqx@ceprei.biz

Keywords: solar cell, split, concentration, diffractive optical element, high efficiency

Abstract. In this paper, a diffractive optical element(DOE) is designed as a spectrum splitting and concentrating element which is used in lateral multi-junction solar cells. The performance of the DOE by simulation indicates that optical efficiency over 80% can be achieved based on this design. The relationship between light concentration ratio and cell efficiency is researched. The results revealed that the cell efficiency increase with the light concentration ratio growing. It indicates that both the spectrum split and concentration realized by DOE is beneficial for the improvement of solar cell efficiency, which provide an important alternative approach to improve photovoltaic efficiency without the necessary need for epitaxial technology widely used in tandem solar cells, and would thus stimulate the research into high efficiency and low cost solar cells.

Introduction

The efficiency of single-junction solar cell has almost reached the theory limitation about 33% which is decided by Shockley-Queisser limit [1- 2]. Further developing high-efficiency and cost-effective solar cell is very important to the large photovoltaic application. The concept “multi-junction solar cells” that absorbs different spectral bands of the solar spectrum by different semiconductors with corresponding bandgaps is considered to be an useful approach to overcome the Shockley-Queisser limit [3-5]. A theoretical efficiency up to 85% can be achieved based on this concept. However, solar cells with efficiencies greater than 40% are dominated by series-connected tandem multi-junction solar cells[6], which have to meet current matching and lattice matching simultaneously and be fabricated with complex and expensive epitaxial growth technology. Another approach named lateral multi-junction solar cells using an optical sub-system to realize spectrum splitting and concentrating function has been proposed [7-12]. In this kind of solar cells, the sunlight is split into different spectral bands by optical elements such as the dichroic mirror, and absorbed by the corresponding solar cells. Besides, concentration is needed to offset the high cost. Holographic systems, which can split and concentrate the sunlight by volume phase modulation of the wave front, have also been proposed by researchers[13,14]. However, in most cases, the functions of the light concentration and the spectrum splitting are realized by separate optical components, which are so expensive and complex that it is not easy to be applied in large-scale application. Therefore, it is very useful to develop a compact and low-cost optical component for spectrum splitting and concentrating. Recently, a single thin planar DOE, which can implement the function of sunlight splitting and concentrating in one direction synthetically by designing its surface-relief structure, was proposed in our recent work[15,16]. The optical efficiency of the DOE under visible light was also discussed. However, to achieve a reasonable photovoltaic efficiency, all factors, including the sunlight concentration still need to be investigated seriously.

In this paper, a DOE architecture is designed as the spectrum splitting and concentrating optical element, which is used in lateral multi-junction solar cells. The performance of the DOE is given by simulation. Simulation results show that the sunlight spectrum can be split and concentrated to predesigned positions well and the corresponding average optical efficiencies for calculated wavelengths can reach over 80% with the maximum thickness of 250 μm . The relationship between light concentration ratio and cell efficiency is researched. The results revealed that the cell efficiency increase with the light concentration ratio growing. As a result, a high-efficient solar cell system can be expected since both spectrum split and concentration function designed in this work can improve the cell efficiency. Since the DOE in our design is appropriate for mass production by using imprint technology, our work provides an economical way for the application of high efficiency lateral multi-junction solar cells.

Model and design method

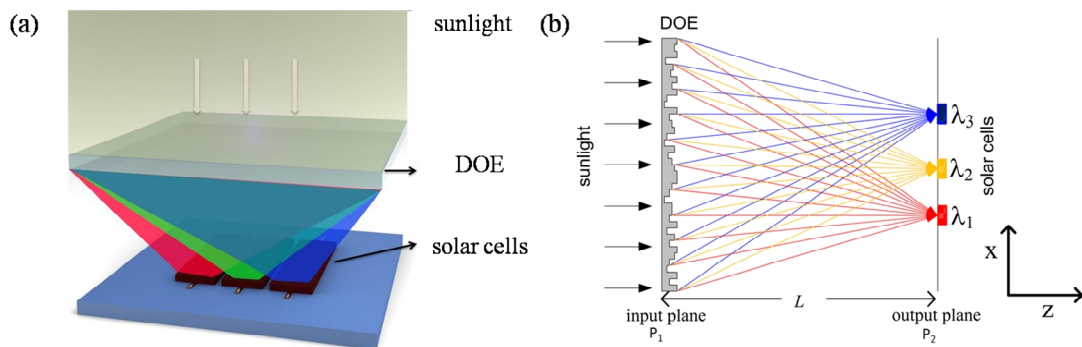


Fig.1 . (a) Scheme of the lateral multi-junction solar cell architecture with DOE as a spectrum splitting solar concentrator. (b) Sectional view of the corresponding architecture, the DOE is used to split and concentrate sunlight in the X direction, and concentrate sunlight in the Y direction. Solar cells with increasing band gaps (E_g) are laterally placed along the X direction in sequence according to the spectrum distribution on the output plane (P_2), the Y direction is perpendicular to the paper and sunlight is incident along the Z direction.

As the DOE can realized various optical functions such as concentration, dispersion and beam shaping by modulating the wavefunction[17-23], the design of the lateral multi-junction solar cells architecture with a DOE as the spectrum splitting solar concentrator is shown in Fig. 1. The incident sunlight is split and concentrated to the predesigned positions by a DOE. Solar cells with different band-gaps are placed at corresponding positions. The DOE is placed in x - y plane and illuminated by sunlight consisting of continuous wavelength components. The incident direction of sunlight is along the z axis. P_1 represents the input plane where the DOE is placed, P_2 represents the output plane where the solar cells are placed, and L represents the distance between P_1 and P_2 . It is well known that the sunlight irradiated on the ground can be viewed as a combination of plane waves. The wave function of the incident sunlight on the surface of the DOE before reflection can be written as [17-19]

$$U_1(x_1, y_1, \lambda) = \rho_1(x_1, y_1, \lambda) \exp[i\Phi_1(x_1, y_1, \lambda)]. \quad (1)$$

where $\rho_1(x_1, y_1, \lambda)$ and $\Phi_1(x_1, y_1, \lambda)$ represent the amplitude and phase of the wave function for wavelength λ at position (x_1, y_1) on P_1 , respectively. The two parameters $\rho_1(x_1, y_1, \lambda)$ and $\Phi_1(x_1, y_1, \lambda)$ are uniform on P_1 for wavelength λ before reflection, i.e. $\rho(x_1, y_1, \lambda) = \rho(\lambda)$ and $\Phi_1(x_1, y_1, \lambda) = \Phi_1(\lambda)$. The designed DOE shown in Fig. 1 is a two-axis concentrator, where the incident light is split and concentrated in x - z plane and concentrated only in y - z plane. In order to better verify the feasibility of this conceptual framework, the design is simplified to 2 dimensions in this work. In other words, the surface-relief structure is designed to split and concentrate the incident light in x - z plane and extended

by extruding the 2 dimensional contours in direction y . In the future work, this design can be extended in the y - z plane to generate a surface-relief just for substantially increasing the attainable concentration.

In actual simulation, the continuous functions can be expressed by a set of discrete values at sampling pixels. The numbers of sampling pixels on P_1 and P_2 are N_1 and N_2 , respectively. The depth of the DOE for k_{th} sampling pixel is h_k . In discretization representation, considering Eq. (1) and the phase modulation by the depth distribution, the wave function distribution of the sunlight on the surface of the DOE after reflection can be expressed as

$$U_{1k}(I) = r_{1k}(I) \exp[i2\pi h_k(n_1 - 1)/I] \quad (2)$$

$k = 1, 2, 3, \dots, N_1,$

The output wave function at m_{th} sampling pixel is related to $U_{1k}(\lambda)$ and a linear transform with Fresnel diffraction integral kernel $G(x_1, x_2; L, \lambda)$ in the form:

$$U_{2m} = \sum_{k=1}^{N_1} \hat{G}_{mk}(I) U_{1k}(I). \quad (3)$$

$m = 1, 2, 3, \dots, N_2.$

The corresponding light intensity of the sunlight at wavelength λ on P_2 is

$$I_2(m, I) = |U_{2m}(m, I)|^2. \quad (4)$$

It indicates that the intensity distribution of the sunlight can be modulated by changing the surface-relief structure of the DOE (i.e., the h_k in Eq.(2)). In this design, the morphology of the DOE is optimized by simulation of the depth distribution of DOE. More specifically, the DOE is designed to spatially split and concentrate light of three wavelengths ($\lambda_1 = 450$ nm, $\lambda_2 = 550$ nm, $\lambda_3 = 650$ nm) at three predesigned positions in sequence, and light of other wavelengths can also be split and concentrated in corresponding positions.

Results and discussion

The parameters of the DOE are given as follows. The distance (L) between P_1 and P_2 is 600 mm. P_1 has the size of 20.00 mm (along direction x) \times 20.00 mm (along direction y). P_1 (DOE) is quantized into 4096 equal sampling pixels along direction x , with the width of each sampling pixel of 4.88 μ m. The maximum depth of the DOE is restrained within 250 μ m. The DOE is designed to spatially split and concentrate three wavelengths ($\lambda_1 = 450$ nm, $\lambda_2 = 550$ nm, $\lambda_3 = 650$ nm) at three predesigned positions on P_2 in sequence. The corresponding focal positions are set to be 5.9 mm, 7.2 mm and 8.5 mm, respectively. Wavelengths (500 nm and 600 nm) are chosen to verify the performance of the designed DOE for other wavelengths. The result is shown in Fig.2a, it shows that different wavelengths ($\lambda_1 = 450$ nm, $\lambda_2 = 500$ nm, $\lambda_3 = 550$ nm, $\lambda_4 = 600$ nm, $\lambda_5 = 650$ nm) are concentrated at five different regions on P_2 according to their wavelengths when the DOE is under illumination. It indicates that those wavelengths except design wavelengths can be split and concentrated well and arranged in sequence.

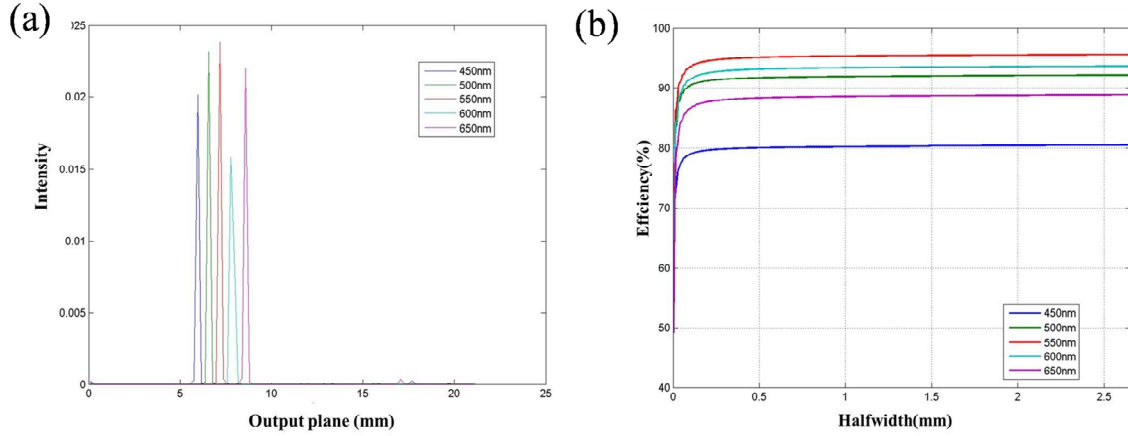


Fig. 2. (a) Simulation results of output light intensity distribution on P_2 , the designed DOE for five wavelengths ($\lambda_1 = 450$ nm, $\lambda_2 = 500$ nm, $\lambda_3 = 550$ nm, $\lambda_4 = 600$ nm, $\lambda_5 = 650$ nm) with maximum depth of $250\mu\text{m}$. (b) Simulation results of the optical efficiency η with different halfwidth for five wavelengths ($\lambda_1 = 450$ nm, $\lambda_2 = 500$ nm, $\lambda_3 = 550$ nm, $\lambda_4 = 600$ nm, $\lambda_5 = 650$ nm).

In order to evaluate the splitting and concentrating performance of the DOE quantitatively, the optical efficiency η for wavelength λ is defined as follow,

$$h(I) = \frac{\int_{x_{2f}-w/2}^{x_{2f}+w/2} |U_2(x_2, I)|^2 dx_2}{\int |U_1(x_1, I)|^2 dx_1} \times 100\% \quad (5)$$

where x_{2f} represents the focal position for wavelength λ on P_2 , the numerator represents the sum of energy in the given region, the half width of the region is defined as $w/2$, the denominator represents the total energy of the incident light for wavelength λ on P_1 . Fig. 4 shows the optical efficiency η for these five wavelengths with different half width.

As shown in Fig. 2b, the optical efficiency for wavelengths reach a high value with half width of ~ 0.1 mm, which means most energy of these five wavelengths is concentrated in a narrow region on P_2 compared with the width of the incident light 20 mm. The optical efficiencies obtained in the simulation for these five wavelengths with half width of 0.1mm are calculated and presented in Table 1.

Table 1. Simulation results of focal positions and optical efficiencies with half width of 0.1mm on P_2 .

	450 nm	500 nm	550 nm	600 nm	650 nm
focal position (mm)	5.9	6.5	7.2	7.8	8.5
Optical efficiency	80.1	90.8	93.3	91.3	85.2

The detailed balance limit, which was proposed by Shockley-Queisser in the 1960s [2], has been used and developed extensively to calculate the limiting efficiency for a single gap solar cell and multi-junction solar cells in various conditions. To simplify the problem, we will directly show how to solve the limiting efficiency by citing the key equations. The theory shown in the following is a general case of Shockley-Queisser limit and can calculate any photovoltaic solar cell with a single uniform band gap, such as p-n junctions and semiconductor-electrolyte interface cell. Detailed discussions and assumptions could be found in those works. Consider a two-level solar cell consisting of electrons in a valence-band and conduction-band, with E_g being the band gap. $I_s(\lambda)$ is the solar radiation flux at wavelength λ in photons /unit bandwidth /unit area /second incident upon the solar cell, which is given

by blackbody radiation expression or experimentally determined data such as ASTM International G173-03 global spectrum (AM1.5G) [24]. The rate of the photon absorption is expressed as

$$R_s = \int S(I) I_s(I) dI, \quad (6)$$

where $\sigma(\lambda)$ is the cross section per unit area of solar cell for absorption of a photon with wavelength λ . $\sigma(\lambda)$ is given by

$$S(I) = \begin{cases} t_s(I) & \text{for } I \leq I_g \\ 0 & \text{for } I > I_g \end{cases}, \quad (7)$$

where $t_s(\lambda)$ is the probability that a photon, which irradiates on the surface with energy greater than the band gap, will be absorbed and produce an electron-hole pair. $t_s(\lambda)$ equals to IPCE(λ) when all electrons stimulated by the light are transported to the external circuit. In most cases and also in this paper, $t_s(\lambda)$ is assumed to be a constant to simplify the problem. based on this assumption, the theory is reduced to the classical Shockley-Queisser limit.

The absorption of photons raises the thermodynamic potential, μ , which refers to the difference between the conduction band and the valence band. Ignoring stimulated emission in such conditions, the rate of radiative decay, $R_D(\mu)$, has been obtained by Ross [25]:

$$R_D(\mu) = L \exp(\mu / kT_c), \quad (8)$$

where T_c is the temperature of the solar cell and where L is given by

$$L = \int S(I) \frac{4pc}{I^4} \exp\left(\frac{-hc}{IkT_c}\right) dI. \quad (9)$$

Substituting Eq. (7) into Eq. (9) with the assumption $t_s(\lambda) = t_s$ provides us an analytical expression for L

$$L = t_s \frac{4pkT_c}{h^3c^2I_g^2} \exp(-hc / I_g kT_c) (h^2c^2 + 2hckT_c I_g + 2k^2T_c^2 I_g^2). \quad (10)$$

The open-circuit potential μ_0 is given by

$$\mu_0 = kT_c \ln(f_i f_c R_s / L + 1), \quad (11)$$

where f_c is the fraction of the electron-hole recombination due to radiative transitions and f_i is the fraction of electron-hole recombination whose released energy is not extracted by the circuit. The power output per unit area of cell is

$$P = (1 - f_i) R_s \mu, \quad (12)$$

and a maximum power output P can be found by solving $\partial P / \partial f_i = 0$. The result is

$$P = V_0 e R_s m(z), \quad (13)$$

where $m(z) = z^2 / [(1+z \cdot \exp(-z))(z + \ln(1+z))]$ and z is the root of the equation $z + \ln(1+z) = \mu_0 / kT_c$. $V_0 = \mu_0 / e$ is the open voltage and $m(z)$ is known as filling factor. So the efficiency can be written as

$$h = V_0 e R_s m(z) / P_s = V_0 e R_s m(z) / \int \frac{hc}{\lambda} I_s(\lambda) d\lambda, \quad (14)$$

where P_s is the total input energy on the solar cell per unit area per second.

Using the equations above, limiting efficiency η for solar cell with band gap E_g under radiation of AM1.5G spectrum is calculated, as shown in Fig. 3(a). Different concentration ratios are plotted in the same figure, and it's obviously that low to medium concentration can raise the efficiency notably. This result is readily comprehensive and functions of z since the increase of I_s will raise R_s and consequently μ_0 , V_0 , z , and $m(z)$ when z is small (Fig. 3(b)). Substituting $I_s(\lambda)$ and E_g with any given radiation flux and a given gap, respectively, we can calculate the limiting efficiency of the solar cell under such radiation.

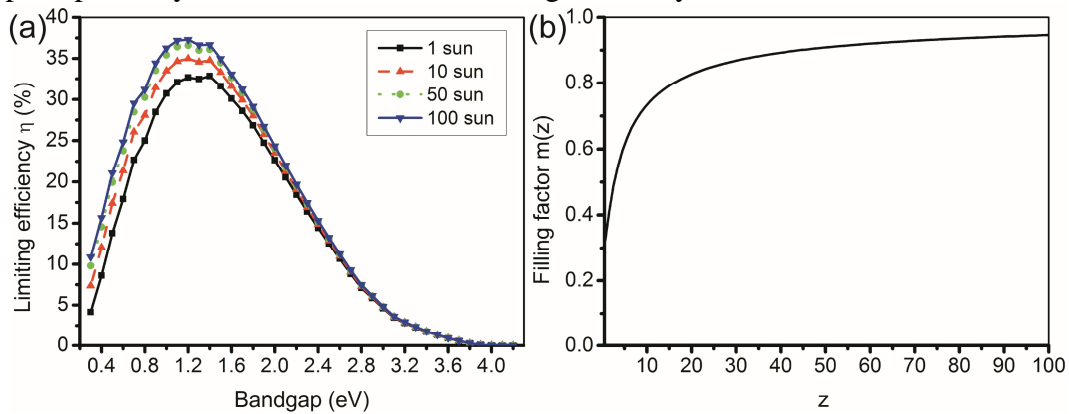


Fig. 3. (a) Limiting efficiency versus band gap under different concentrations of AM1.5G spectrum irradiation. (b) Filling factor $m(z)$ versus z .

Obviously, the light concentration can improve the solar cell efficiency at any given bandgap. The limiting efficiency curve indicates that the total efficiency can be promoted by a combination of cells with different bandgap. As a result, the DOE designed in this work which can realize spectrum splitting and concentrating functions simultaneously provide a potential approach for high-efficiency and cost-effective solar cells.

Conclusions

A thin DOE with the functions of spectrum splitting and concentrating has been designed. The maximum depth of the designed DOE is 250 μm . We simulated the spectrum splitting and concentrating performance quantitatively. The simulation results revealed that the DOE can successfully split and concentrate the design wavelengths and other wavelengths onto the predesigned positions. The optical efficiency can reach a very high level over 80%. The limiting efficiency curve indicates that the total efficiency can be promoted by a combination of cells with different bandgap. A reasonable speculation can be obtained that the DOE present a “rainbow-like” pattern under actual solar illumination, which can be adapted to different sets of solar cells including commercialized silicon solar cells and tandem solar cells and the corresponding theory efficiency can be estimated based on the results in this work. A highly-efficient single and compact DOE will offer a valuable contribution to the development of high efficiency and cost-effective lateral multi-junction solar cells.

Acknowledgements

The authors appreciate the financial support of the Major Science and Technology Projects of Guangdong Provincial Science and Technology Department (NO. 2015B010114002) and

the Collaborative Innovation Projects of Guangdong Provincial Science and Technology Department(NO. 2014B040404046).

References

- [1] M. A. Green, K. Emery, Y. Hishikawa, W. Warta, and E. D. Dunlop, *Prog. Photovoltaics Res. Appl.* 20, 12-20 (2012).
- [2] W. Shockley and H. J. Queisser, *J. Appl. Phys.* 32, 510-519 (1961).
- [3] M. A. Green and A. Ho-Baillie, *Prog. Photovoltaics Res. Appl.* 18, 42-47 (2010).
- [4] J. D. McCambridge, M. A. Steiner, B. L. Unger, K. A. Emery, E. L. Christensen, M. W. Wanlass, A. L. Gray, L. Takacs, R. Buelow, and T. A. McCollum, *Prog. Photovoltaics Res. Appl.* 19, 352-360 (2011).
- [5] A. Polman and H. A. Atwater, *Nat. Mater.* 11, 174-177 (2012).
- [6] Yuen. H, in *Renewable Energy and the Environment*, OSA Technical Digest (CD) (Optical Society of America, 2011) paper SRWB3(2011).
- [7] E. D. Jackson, "Solar energy converter," U.S. Patent 2,949,498 (1960).
- [8] A. Barnett, D. Kirkpatrick, C. Honsberg, D. Moore, M. Wanlass, K. Emery, R. Schwartz, D. Carlson, S. Bowden, and D. Aiken, *Prog. Photovoltaics Res. Appl.* 17, 75-83 (2009).
- [9] A. Imenes and D. Mills *Sol. Energy Mater. Sol. Cells.* 84, 19 (2004)
- [10] J. Ludman *Am. J. Phys.* 50, 244 (1982)
- [11] A. Barnett, D. Kirkpatrick, C. Honsberg, D. Moore, M. Wanlass, K. Emery, R. Schwartz, D. Carlson, S. Bowden, and D. Aiken, presented at the 22nd European photovoltaic solar energy conference, Milan, Italy, 3 September 2007,
- [12] B. Mitchell, G. Peharz, G. Siefer, M. Peters, T. Gandy, J. C. Goldschmidt, J. Benick, S. W. Glunz, A. W. Bett, and F. Dimroth, *Prog. Photovoltaics Res. Appl.* 19, 61-72 (2011).
- [13] D. Vincenzi, A. Busato, M. Stefancich, and G. Martinelli, *Phys. Status. Solidi.* 206, 375-378 (2009).
- [14] M. Stefancich, A. Zayan, M. Chiesa, S. Rampino, D. Roncati, L. Kimerling, and J. Michel, *Opt. Expr* 20, 9004-9018 (2012).
- [15] Huang Q, Wang J, Quan B, Zhang Q, Zhang D, Li D, Meng Q, Pan L, Wang Y and Yang G *Appl. Opt.* 52, 2312 (2013)
- [16] Ye J, Wang J, Huang Q, Dong B, Zhang Y and Yang G *Chin. Phys. B* 22, 34201 (2013)
- [17] B. Y. Gu, G. Z. Yang, B. Z. Dong, M. P. Chang, and O. K. Ersoy, *Appl. Opt.* 34, 2564-2570 (1995).
- [18] B. Z. Dong, G. Q. Zhang, G. Z. Yang, B. Y. Gu, S. H. Zheng, D. H. Li, Y. S. Chen, X. M. Cui, M. L. Chen, and H. D. Liu, *Appl. Opt.* 35, 6859-6864 (1996).
- [19] Y. Ogura, N. Shirai, J. Tanida, and Y. Ichioka, *J. Opt. Soc. Am. A* 18, 1082-1092 (2001).
- [20] M. W. Farn, M. B. Stern, W. B. Veldkamp, and S. S. Medeiros, *Opt. Lett.* 18, 1214-1216 (1993).
- [21] A. Herbjornrod, K. Schjolberg-Henriksen, H. Angelskar, and M. Lacolle, *Journal of Micromechanics and Microengineering* 19(2009).
- [22] H. Angelskar, I. R. Johansen, M. Lacolle, H. Sagberg, and A. S. Sudbo, *Opt. Express* 17, 10206-10222 (2009).
- [23] O. Lovhaugen, I. R. Johansen, K. A. H. Bakke, B. G. Fismen, and S. Nicolas, *Journal of Modern Optics* 51, 2203-2222 (2004).
- [24] I.E. Commission, *I. Internat ional Standard, Edition 2* , ISBN 2 –8318 –9705-X, (2008)
- [25] R. Ross, *J. Chem. Phys.*, 46, 4590-4593 (1967)